# An Efficient Technique for the Optimization of Submillimeter-wave Schottky-diode Harmonic Multipliers

Chih-Chien Lee[1], Boris Gelmont[1] and Dwight Woolard[2]

[1]The University of Virginia
Electrical Engineering Department
Charlottesville, VA 22903

[2]U.S. Army Research Laboratory
U.S. Army Research Office
Research Triangle Park, NC 27709

**Abstract**

A simple and efficient modified harmonic-balance technique is presented. This new algorithm is suitable for the large-signal time-dependent analysis of nonlinear millimeter wave circuits. The accurate design and successful implementation of very high frequency nonlinear circuits requires both a detailed understanding of the physical operation of the active devices and of how these nonlinear devices interact with the linear embedding circuit. This work addresses the specific task of establishing a robust simulation tool that combined this novel modified harmonic-balance circuit analysis technique with a physics-based hydrodynamic transport model device simulator. A comparison with the accelerated fixed-point (AFP) harmonic-balance technique has been made through an evaluation of a Schottky-diode multiplier. The result shows that this approach can be used to realize improved multiplier operation with a minimal time of numerical computation.

## I. INTRODUCTION

The development of computer-aid analyses of highly nonlinear circuits requires both a detailed understanding of the physical operation of the active devices and of how these nonlinear devices interact with the linear embedding circuit. Traditionally, the nonlinear active devices are modeled by the lumped quasi-static equivalent circuit analysis. However, this equivalent circuit model has lost validity at higher frequency millimeter wave where the large-signal nonstationary phenomena begin to dominate device operation. It is clearly that a physics-based numerical device model is required for the active device analysis. In an earlier investigation, drift-diffusion and Monte Carlo based harmonic-balance algorithms have been utilized. The drift-diffusion model is a low-order approximation of the Boltzmann transport equation, it implies that mobility of the carrier is only a function of the local electrical field and it does not take account of the non-stationary characteristics such as carrier heating and velocity overshoot. The Monte Carlo simulation has difficulty in treating low-field region. Also, the statistical noise in the solution and the intensive amount of computation time required make this model impractical for device design. An alternative approach is hydrodynamic transport model, which is obtained by taking the first three moments of the Boltzmann Transport Equation [1]. Comparing to quasi-static equivalent circuit and drift-diffusion model, hydrodynamic model is more accurately in treating high-field, nonstationary, and hot-electron effects.

The specific focus of this paper is on energy transport effects and their influence on the harmonic multiplication within reversed-bias Schottky-barrier varactor diodes. Equally important to the characterization of diode multipliers is the optimization of the nonlinear element to the externally coupled embedding impedance. Here, the second-harmonic power (i.e., current and voltage) of the matched diode is optimized before constraints on embedding impedance, local voltage and dc bias are specified. The key of this approach is the reduction of systems variables by an efficient mathematical ordering of the optimization procedure. Specifically, this new method reduces the typical optimization problem (i.e., where device and circuit are considered simultaneously) for a doubler, where 2 harmonics are considered, from n+2 variables to n variables. As will be shown, this approach leads to a significant computational advantage for Schottky-diode multiplier design.

In this paper, a one-dimensional time-dependent simulation algorithm is presented which employs a fully hydrodynamic transport equation [1,2] with two-valley mobility model to describe the diode physics within the depletion and bulk regions. These studies assume a reversed-biased situation and employ appropriate boundary conditions at the barrier interface. In addition, this work combines the physically accurate diode model with a modified harmonic-balance algorithm to determine diode-circuit designs that maximize power generation and/or power efficiency in the second harmonic [2]. The modified harmonic-balance method utilizes a novel two-step procedure where the available doubler-power and the second-harmonic diode-impedance is first derived as a function of first and second harmonic diode excitation. The harmonic diode-voltages and second-harmonic diode-impedance at the optimum power-point are then used to define the matched embedding impedance and the optimum local-oscillator (LO) voltage. The utility of this simulation tool is illustrated by comparing to prior studies, by others, that employed traditional drift-diffusion transport models, Monte Carlo transport models and a conventional harmonic-balance algorithm. Specifically, this work demonstrates a computationally efficient and accurate physical description as well as a more robust approach for circuit optimization.

## II. PHYSICS-BASED DIODE MODEL

These multiplier studies utilize a physics-based Schottky-diode model accurate for both momentum and energy relaxation effects. Here, a one-dimensional time-dependent simulation algorithm is implemented that employs a fully hydrodynamic transport model (i.e. first three moments of the Boltzmann equation) to describe the diode physics within the depletion and neutral regions. The application this type of approach will be necessary for GaAs diodes operating at terahertz frequencies because energy relaxation is important above 300 GHz and momentum relaxation is important above 1 THz. While our method is fully amenable to momentum relaxation these initial studies will consider device operation below 1 THz. These studies consider the large-signal operation of a Schottky-barrier

varactor frequency multiplier and will therefore consider diodes under time-dependent reverse-bias up to the breakdown voltage.

Set of equations of the hydrodynamic model in the single-gas approximation has been written in [1,2] together with appropriate boundary conditions. We have used in [2] one valley approximation. However more adequate description of GaAs Schottky diodes can be obtained utilizing a two-valley model [3]. We' ll extract the mobility and the energy relaxation time from this model.

Consider a semiconductor material whose energy band structure can be approximated by a two-valley model with an energy separation $\Delta_{UL}$ between the upper and lower valleys. The collision terms are modeled by the relaxation-time approximation. The energy collision term is expressed as

$$(\frac{\P w_n}{\partial t})_c = -\frac{w_n - w_0}{t_w}, \tag{1}$$

where $w_o = 3k_B T_o/2$ is the equilibrium energy at the lattice temperature $T_o$ , $t_w$ is the energy relaxation time, $k_B$ is the Boltzmann constant. The average electron total energy $w_n$ is defined using the thermal approximation

$$w_n = \frac{3}{2}k_B T_e + h\Delta_{UL} \tag{2}$$

where $T_e$ is the electron temperature, $h$ is the fraction of the electrons in the upper valley. The energy separation between the upper and lower valleys $\Delta_{UL}$ is set to 0.29 eV in this work. The total energy relaxation time is given by

$$\frac{1}{t_w} = \frac{1-h}{t_{w\mathrm{L}}} + \frac{h}{t_{w\mathrm{U}}}. \tag{3}$$

The energy relaxation time in the lower-valley and upper-valley are $\tau_{wL}$=1.5 ps and $\tau_{wU}$=0.8 ps, respectively. The fraction of the electrons in the upper valley and is given by

$$h = \frac{n_{\mathrm{U}}}{n_{\mathrm{U}} + n_{\mathrm{L}}} = \frac{r}{r+1} \tag{4}$$

where $n_{\mathrm{L}}$ and $n_{\mathrm{U}}$ are the electron densities in the lower valley and upper valley. The ratio of electron densities $r$ is defined as

$$r = \frac{n_{\mathrm{U}}}{n_{\mathrm{L}}} = \left( \frac{m_{\mathrm{U}}}{m_{\mathrm{L}}} \right)^{3/2} \exp\left( -\frac{\Delta_{\mathrm{UL}}}{k_B T_e} \right) \tag{5}$$

where $m_{\mathrm{L}}$ and $m_{\mathrm{U}}$ are the density-of-states effective masses of lower valley and upper valley are set equal to 0.063 $m_0$ and 0.55 $m_0$, respectively. The temperature dependent electron mobility is obtained by

$$m_n = (1-h) m_{\mathrm{L}} + h m_{\mathrm{U}} . \tag{6}$$

where $m_{\mathrm{L}}$ and $m_{\mathrm{U}}$ are the electron mobility in the lower valley and upper valley, respectively. The mobility can be approximated by [4,5]

$$m_{\mathrm{L}} = \frac{m_{0\mathrm{L}}}{1 + 3 k_B g_{\mathrm{L}} (T_e - T_0)/2}, \quad g_{\mathrm{L}} = \frac{m_{0\mathrm{L}}}{q t_{w\mathrm{L}} v_{sat\mathrm{L}}^2} \tag{7}$$

and

$$m_{\mathrm{U}} = \frac{m_{0\mathrm{U}}}{1 + 3 k_B g_{\mathrm{U}} (T_e - T_0)/2}, \quad g_{\mathrm{U}} = \frac{m_{0\mathrm{U}}}{q t_{w\mathrm{U}} v_{sat\mathrm{U}}^2} \tag{8}$$

where the saturation velocities for lower-valley $v_{sat\mathrm{L}}$ and upper-valley $v_{sat\mathrm{U}}$ are set equal to $3.2\times10^5$ m/s and $1.\times10^5$ m/s, respectively. These values were obtained by fitting Monte Carlo simulation results. The low-field, doping-dependent mobility for two valleys are expressed as [1]

$$m_{0\mathrm{L}} = \frac{m_{00\mathrm{L}}}{1 + [\log(N_T)/B_{\mathrm{L}}]^n}, \qquad m_{0\mathrm{U}} = \frac{m_{00\mathrm{U}}}{1 + [\log(N_T)/B_{\mathrm{U}}]^n} \tag{9}$$

where $N_T$ is the total doping density (here total ionization is assumed, so $N_T = N_D$). Here, $m_{00\mathrm{L}}$=0.85 m$^2$/V-s, $m_{00\mathrm{U}}$=0.26 m$^2$/V-s [6], $n$ = 23, and $B_{\mathrm{L}}$=23, and $B_{\mathrm{U}}$=26 are used.

As to boundary conditions discussed in [2] we have to change the phenomenological energy-flux boundary condition

$$S_n(0^+) = v_M \, n_M \, d \, k_B \, T_0 - v_S \, n(0^+) (d \, k_B \, T_e(0^+) + h\Delta_{UL}), \tag{10}$$

where $\delta = 2.5$ is used.

## III. VARACTOR FREQUENCY-MULTIPLIER NUMERICAL SIMULATION

While an accurate model for the physical diode is very important as one attempts to design varactor multipliers at very high frequencies, the ability to effectively couple the device to

the proper embedding impedance is of paramount importance. In fact, the majority of the analytical and numerical effort involved in realizing efficient multipliers is expended in the matching of the nonlinear device to the embedding circuit [7]. For example, many harmonic-balance methods have been derived (e.g., multiple-reflection algorithm [8] and accelerated fixed point [9]) to improve the matching of the various harmonics between nonlinear device and linear circuit. Here the difficulty lies in the large number of iterations that are required to optimize power-efficiency of a given nonlinear element over both embedding impedance and local oscillator (LO) voltage. This problem becomes compounded for optimization over the physical diode design and in circuits that contain many nonlinear device elements. Of course, in some situations where multiple diodes are involved equivalent-circuits can be developed that reduce groups of diodes to a single nonlinear element [10].

When a conventional harmonic-balance (HB) algorithm is applied to the analysis of a varactor-doubler the problem is to optimize the second-harmonic generation. Here, embedding impedances are selected for the first- and second-harmonic circuits and short-circuit conditions are assumed at the higher harmonics. While there are many HB techniques one of the most popular is the multiple-reflection algorithm [8] that seeks to smooth transients via the introduction of a loss-less transmission-line section. This relaxation method, which in some cases requires long convergence times, has been improved by Tait [9]. Regardless of the exact mathematical algorithm employed, the primary challenge in the design of a doubler is to determine the embedding impedance that will yield the maximum second-harmonic power. In the conventional approach, the physical model of the Schottky diode is used in conjunction with the HB algorithm to optimize the second-harmonic power. Specifically, the HB technique will iterate between the Fourier-domain solutions of the circuit(s) and the current/voltage harmonics derived from steady-state time-domain simulations of the diode. Since this combined Fourier-domain and time-domain analysis inevitably leads to extensive iterations and to a large computational cost, it is natural to seeks alternative methods that reduce the numerical burden of the optimization task. In the simulations presented here, a new two-step procedure has been utilized to achieve this goal. This modified HB algorithm introduces a new optimization constraint that enables a natural separation of the device-circuit problem. Specifically, this procedure allows the current/voltage harmonics of the nonlinear device to be optimized independently of the external circuit. Subsequently, the optimum embedding circuit can then be derived from a very simple analysis.

### *Harmonic-Balance Technique*

The harmonic-balance circuit analysis applied in this paper is the accelerated fixed-point (AFP) method [9]. The iterative process is repeated until the harmonic components of the voltage converge to within a specified tolerance factor of their steady-state value for all harmonics. In this work, the tolerance is set to 0.1%. There is one thing to remind that AFP algorithm has one adjustable convergence parameter $Z_0$, the fictitious transmission

line characteristic impedance. The chosen value of $Z_0$ can affect the convergence property of the iteration.

***Modified Harmonic-Balance Technique***

The key to this simplified approach is to formulate the optimization-problem of the varactor-doubler in a completely different way. Specifically, to recognize that the available-power of the diode at the doubler-frequency may be optimized a priori (i.e., independent of the external circuit) and that the Fourier results can be used, subsequently, to determine the embedding impedance and LO voltage. While this technique represents, in a manner of speaking, an inverse transformation of the conventional problem, it is completely valid and offers definite computational advantages. The technique has been outlined in [2].

In present analysis we have included the frequency-dependent parasitic impedances as additional contributions to the linear device embedding circuit. It is important to note that the parasitic impedances of interested here are external to the active region of the nonlinear device. The matching embedding impedances are given by

$$Z_n^{Circuit} = Z_n^{Linear} - Z_n^{Parasitic} . \tag{11}$$

where $Z_n^{Linear}$ are the matching linear impedances determined using equations from [2].
The power incident from the pump at the input port is

$$P_{in} = V_{C1} I_{C1} / 2 + (I_{C1}^2 + I_{S1}^2) Re\{Z_1^{Parasitic}\} / 2 . \tag{12}$$

The power delivered to port 2 with impedance $Z_2^{Circuit}$ is

$$P_{output} = -\left(V_{C2} I_{C2} + V_{S2} I_{S2}\right)/2 - (I_{C2}^2 + I_{S2}^2) Re\{Z_2^{Parasitic}\} / 2 \tag{13}$$

where $V_{C1}$, $V_{C2}$ and $V_{S2}$ are the dc, first, and second harmonic voltages, respectively. The current harmonics $I_{C1}$, $I_{C2}$, $I_{S1}$ and $I_{S2}$ are supplied by Fourier transforms of time-domain simulations from the physical diode model.

Note that this new approach offers an immediate reduction in problem complexity as compared to the conventional HB approach. Specifically, the traditional HB method will maximize the nonlinear diode-circuit problem over LO voltage (dc and ac) and over the real and imaginary parts of the first- and second-harmonic embedding impedance which is a six-dimensional space. It should be noted that this reduction from N to N-2 in the double problem also occurs in the analysis of a varactor-tripler due to symmetry considerations. As shown, the traditional HB technique requires two iterations. For each mapping over the six-dimensional LO-impedance space, one must perform convergent iteration to

balance the harmonics between the embedding impedance and the nonlinear device. On the other hand, the modified method invokes allowable constraints on the available diode power and the embedding impedance(s) (i.e., are always matched to the diode impedance) to reduce the optimization space by two variables. Furthermore, this method only requires a trivial calculation in the second step to derive the final impedance(s) and the LO voltage. In simplest terms reducing the degrees of freedom allows for a significant reduction in computation.

## IV. SIMULATION RESULTS

Both harmonic-balance and modified harmonic-balance simulations were utilized with the hydrodynamic diode model to study Schottky diode multiplier operation at a doubler-frequency of 200 GHz. Here, the earlier varactor diode investigations that were presented in [11] were considered for comparison purposes. The GaAs Schottky diode considered was UVA-6P4 with an epitaxial doping density of $n_D \approx 3.5\times 0^{16}$ cm$^{-3}$, epitaxial thickness of 1.0 μm, anode diameter 6.3 μm. Experimental results including input power and dc bias were obtained from [12] and were used as the input data for both algorithms. Frequency-dependent parasitic impedances of the UVA 6P4 varactor we used here are similar to those of [8].

### *Harmonic-Balance Technique*

Since we want to compare our result with Monte Carlo transport model, we have the same constraints as [11]. The following constraints are set on the embedding circuit impedances

$$Z_1^{Circuit} = R_1^{Circuit} + jX_1^{Circuit}, \qquad Z_2^{Circuit} = R_1^{Circuit} + j\frac{X_1^{Circuit}}{2}. \tag{14}$$

The embedding impedances of higher harmonics were taken equal to zero. The optimized results obtained from the hydrodynamic model for four simulated input powers are shown in Table I. The simulated result for output power versus incident pump power is shown in Fig. 1. The experimental result and simulated results obtained from the drift-diffusion (DD) and Monte Carlo simulators [11] are also shown in this figure. As seen in this figure, the drift-diffusion model with dc field-dependent mobility is not suitable for high frequency. Since the drift-diffusion model with constant ac mobility did not include the velocity saturation effects, it overpredicted at high input power. The optimal power results of the hydrodynamic model are in good agreement with the result obtained from the simulation of the drift-diffusion model with constant ac mobility at low input power and the result derived from the Monte Carlo simulation at high input power. The output current and voltage waveforms for 18.8 mW pump excitation are shown in Fig 2.

Table I. AFP Harmonic-Balance simulation result by hydrodynamic model

| Incident Pump Power (mW) | Output Power (mW) | $P_{out}/P_{in}$ (%) | $Z_1$ (Ω) | $Z_2$ (Ω) |
|---|---|---|---|---|
| 7.5 | 3.06 | 40.85 | 31+ *j* 207 | 31+*j*103.5 |
| 18.8 | 7.69 | 40.92 | 47+ *j* 234 | 47+*j*117 |
| 29.6 | 9.55 | 32.27 | 61+ *j* 234 | 61+*j*117 |
| 47.0 | 11.91 | 25.34 | 73+ *j* 254 | 73+*j*127 |

***Modified Harmonic-Balance Technique***

The optimized results obtained from the modified harmonic-balance technique hydrodynamic model for four simulated input powers are given in Table I I The optimized results are better than the results from the harmonic-balance (AFP) technique as shown in Fig 3. As seen in the figure, the modified harmonic-balance technique got higher optimized results than the harmonic-balance (AFP) technique. Unlike the traditional HB technique where the fictitious transmission line characteristic impedance has to be carefully chosen, there is no fictitious impedance needed in the modified HB technique. The output current and voltage waveforms for Modified Harmonic-balance method is shown in Fig .4.

Table II. Modified Harmonic-Balance simulation result by hydrodynamic model

| Incident Pump Power (mW) | Output Power (mW) | $P_{out}/P_{in}$ (%) | $V_{LO}$ (V) | $Z_1$ (Ω) | $Z_2$ (Ω) |
|---|---|---|---|---|---|
| 7.5 | 3.23 | 43.10 | 1.062 | 18.7+ *j*199.4 | 46.2+*j*97.2 |
| 18.8 | 8.06 | 42.89 | 1.945 | 25.1+ *j*229.6 | 68.8+*j*116.0 |
| 29.6 | 9.83 | 33.22 | 2.759 | 32.1+ *j*227.7 | 81.5+*j*120.8 |
| 47.0 | 12.08 | 25.71 | 4.025 | 43.0+ *j*240.5 | 86.3+*j*133.6 |

The comparison of results by two techniques shows that the efficiency is a rather flat function of the second harmonic embedding resistance if the first harmonic resistance is matched in appropriate way.

## V. CONCLUSIONS

In conclusion, a simple and efficient modified harmonic-balance technique is presented. This new algorithm is suitable for the large-signal time-dependent analysis of nonlinear millimeter wave circuits. A robust simulation tool that combined this novel modified harmonic-balance circuit analysis technique with a temperature-dependent hydrodynamic transport model device simulator has been established in this paper. In comparison to the drift-diffusion model, this temperature-dependent hydrodynamic model can more accurately describe the nonstationary high frequency dynamics and velocity saturation of

the electron. In addition, the computational time is much reduced over that of the Monte Carlo method. The results and simulation-time requirements for a Schottky-diode multiplier study have been compared to that utilizing the harmonic-balance algorithms. These results show that this approach can be used to realize improved multiplier operation with a minimal time of numerical computation. This model will be used in the future to optimize multiplier operation at terahertz frequencies.

The authors wish to acknowledge the support of the U.S. Army Research Laboratory, Army Research Office.

## REFERENCES

[1] H. Hjelmgren, "Numerical Modeling of Hot Electrons in n- GaAs Schottky-Barrier Diodes," *IEEE Transactions on Electron Devices*, **37**, pp. 1228-1234, 1990.

[2] C. C. Lee, B. L. Gelmont, D. L. Woolard and C. Fazi, "A Modified Harmonic-Balance Analysis of Schottky Diode Multipliers Based upon A Hydrodynamic Transport Model," *Proc. Tenth Int. Symp. on Space Terahertz Technology*, Charlottesville, USA, pp. 313-328, 1999.

[3] K. Bløtekjær, "Transport Equations for Electrons in Two-Valley semiconductors," *IEEE Transactions on Electron Devices*, ED-**17**, pp. 38-47, 1970.

[4] W. Hänsch and M. Miura-Mattausch, "The Hot-Electron Problem in Small Semiconductor Devices," *J. Appl. Phys.*, **60**, pp. 650-656, 1986.

[5] Y. Zhang and M. E. Nokali, "A Hydrodynamic Transport Model and Its Applications in Semiconductor Device Simulation," *Solid-State Electronics*, **36**, pp. 1689-1696, 1993.

[6] M. Shur, *GaAs Devices and Circuits*, (Plenum Press, 1987).

[7] S. A. Maas, *Nonlinear Microwave Circuits*, (Artech House, MA, 1988).

[8] P. H. Siegel, A. R. Kerr, and W. Hwang, "Topics in the Optimization of Millimeter-Wave Mixers," *NASA Technical Papers*, no. 2287, 1984.

[9] G. B. Tait, "Efficient Solution Method for Unified Nonlinear Microwave Circuit and Numerical Solid-State Device Simulation," *IEEE Microwave Guided Wave Letters*, **4**, pp. 420–422, 1994.

[10] M. T. Faber, J. Chramies and M. E. Adamski, *Microwave and Millimeter-Wave Diode Frequency Multipliers*, (Artech House, MA, 1995).

[11] R. E. Lipsey, S. H. Jones, J. R. Jones, T. W. Crowe, L. F. Horvath, U. V. Bhapkar, and R. J. Mattauch, "Monte Carlo Harmonic-Balance and Drift-Diffusion Harmonic-Balance Analysis of 100-600 GHz Schottky Barrier Varactor Frequency Multipliers," *IEEE Transactions on Electron Devices*, **44**, pp. 1843-1850, 1997.

[12] T. W. Crowe, W. C. B. Peatman, R. Zimmermann, and R. Zimmermann, Consideration of velocity saturation in the design of GaAs varactor diodes," *IEEE Microwave Guided Wave Lett.*, Vol. 3, pp. 161-163, 1993.

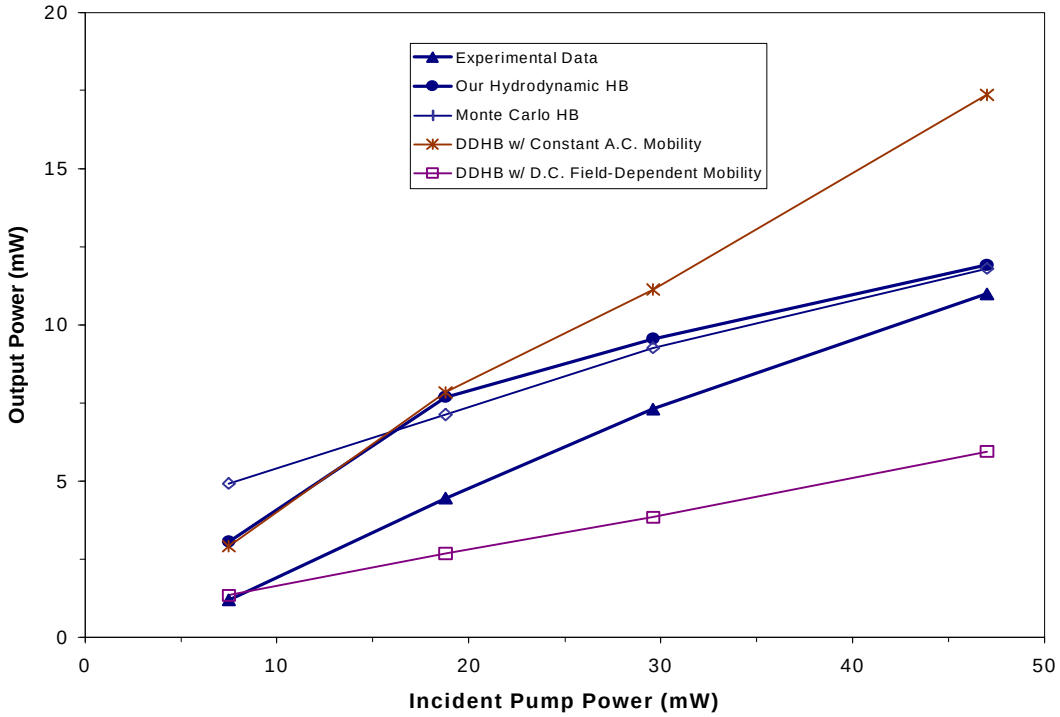


Figure 1. Experimental and AFP theoretical second harmonic output power versus incident pump power for the UVA 6P4 frequency doubler subject to 100 GHz excitation.

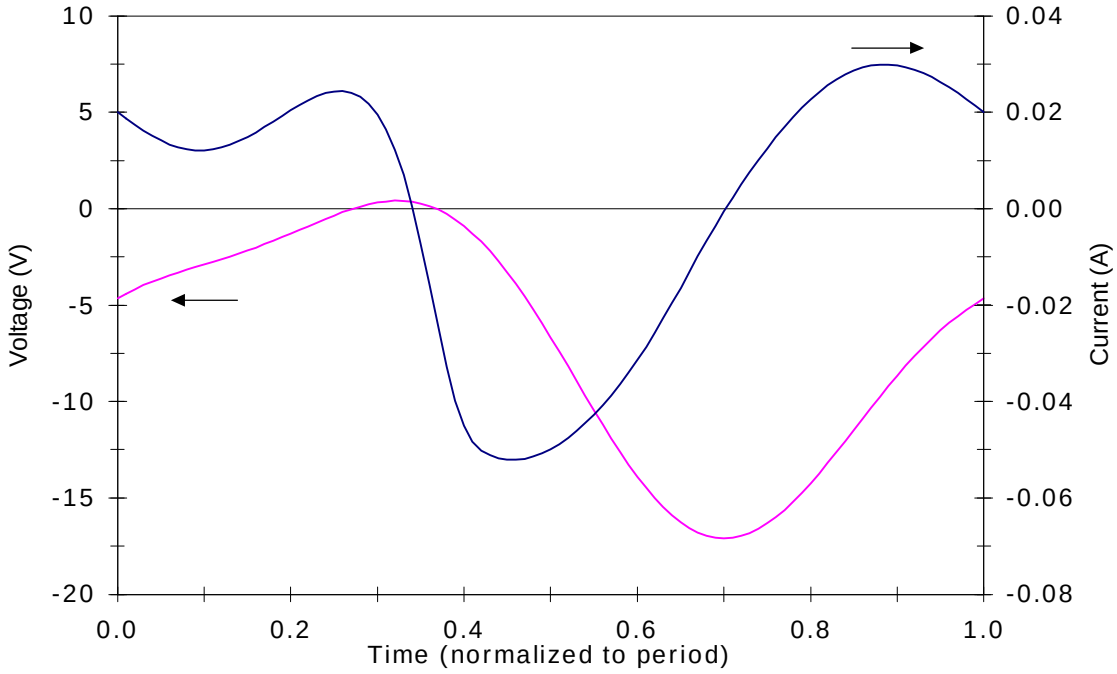


Figure 2. AFP Harmonic-balance current and voltage waveforms for 18.8 mW pump excitation.

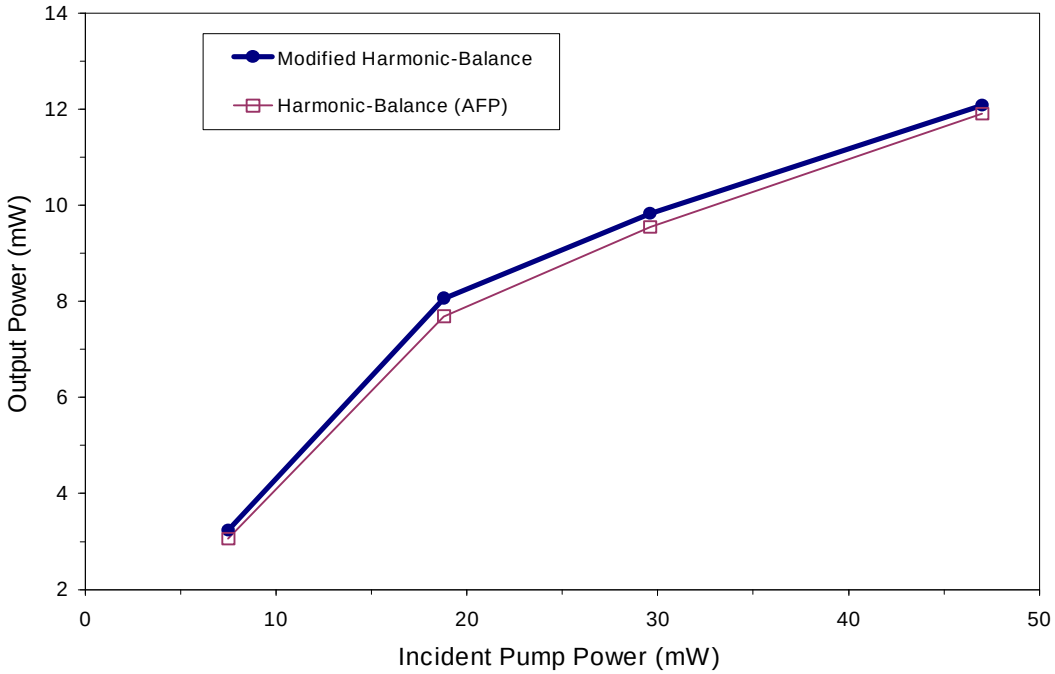


Figure 3. Theoretical second harmonic output power versus incident pump power for the Modified Harmonic-Balance method and Harmonic-Balance (AFP) method.

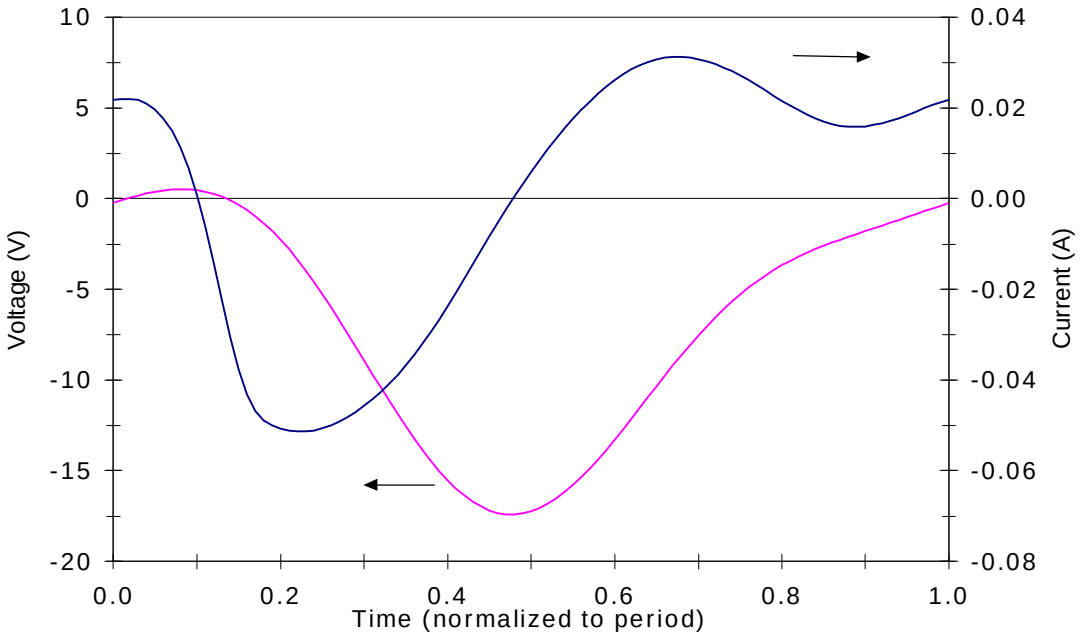


Fig.4. Modified Harmonic-balance current and voltage waveforms for 18.8 mW pump excitation.